Space Weather Throughout the Heliosphere

Article · November 2012

DOI: 10.1063/1.4768751

9 authors, including:

Thomas Detman

James Intriligator
Tufts University

Murray Dryer
Space Weather Predictions Center, Boulder, CO, Unied States iretired)

Wei Webber
National Taiwan University

Space Weather Throughout the Heliosphere

Devrie S. Intriligator [1], Thomas Detman[1], James Intriligator [1,2], Murray Dryer [1], Wei Sun[1,3], Charles Deehr[1,3], William R. Webber[4], Robert B. Decker[5], and Robert L. McPherron[6]

1. Carmel Research Center, P.O. Box 1732, Santa Monica, CA 90406, USA
2. Bangor University, Bangor, Wales, LL572AS, UK
3. Geophysical Institute, University of Alaska, Fairbanks, AK 99775, USA
4. New Mexico State University, Las Cruces, NM 88005, USA
5. Johns Hopkins Applied Physics Laboratory, Laurel, MD 20723, USA
6. University of California Los Angeles, Los Angeles, CA 90095, USA

Abstract. We have analyzed space weather throughout the heliosphere using the three-dimensional (3D) time-dependent magnetohydrodynamic (MHD) Hybrid Heliospheric Modeling System with Pickup Protons (HHMS-PI) [1] out to Voyager 2 (V2) and beyond by comparing the HHMS-PI model results with the available spacecraft data. We also have analyzed space weather throughout the heliosphere through in-depth analyses of the available simultaneous data from a number of instruments on spacecraft at various locations. In this paper we focus on our HHMS-PI modeling (starting at the Sun) of the Halloween 2003 solar events by comparing the model results with spacecraft data at ACE and Ulysses. For the Halloween 2003 solar events we also summarize our inter-comparisons of the in-situ V2 data from many of the V2 instruments. These analyses of the comparisons ("benchmarking") of HHMS-PI simulations and the various spacecraft data and of our in-depth analyses of the V2 particle and field data indicate that particle acceleration and other important physical processes are associated with the heliospheric propagation of these large solar cycle 23 space weather events. We conclude that space weather, originating at the Sun, can have important affects throughout the heliosphere to distances as great as 73 AU and beyond.
Keywords: solar variability effects, solar wind plasma & fields, interplanetary magnetic fields, interplanetary propagation, heliosphere interstellar medium interaction, shocks, pickup ions, energetic particles, cosmic rays
PACS: 96.60.Q.-, 96.50sh, 96.50-e, 96.50.Bh, 96.50Xy,96.50Ya,96.60

INTRODUCTION

Space weather effects extend throughout the heliosphere. Our 3D time-dependent MHD HHMS-PI (Detman et al., 2011 [1]; Intriligator et al., 2012 [2]) model runs out to V2 in the outer heliosphere (OH). In HHMS-PI the lower boundary condition (BC) at 0.1 AU is driven by solar data via the Wang-Sheeley-Arge source surface (SS) current sheet (CS) model [3]. The 3D MHD time-dependent HHMS-PI has two input tracks: the background solar inputs; and the solar event inputs [1, 2]. HHMS-PI is a two-fluid model. It models the SW that flows outward from the Sun; pickup protons (PUPs) created by the ionization of local interstellar medium (LISM) neutral hydrogen (H) flowing into the heliosphere; and their interaction, that slows and heats the SW.

HHMS-PI includes the total energy delivered by PUPs. Previous work used either a polytrope index or generic heat flux to match observed SW temperatures. Waves generated by the scattering of new PUPs feed into a turbulent (Kolmogorov) spectral cascade that dissipates into heating SW protons. Approximately 1% of PUP energy is so transferred to the SW. We are modifying HHMS-PI to include various

SPACE WEATHER: THE SPACE RADIATION ENVIRONMENT
AIP Conf. Proc. 1500, 100-108 (2012); doi: 10.1063/1.4768751

inflowing H models, turbulence, and heating models. The scientific results from HHMS-PI include: good quantitative agreement with SW/IMF data from ACE, Ulysses, and Cassini; quantitative agreement with Ulysses (SWICS) and Cassini (CHEMS) PUP data; pickup protons slow propagating shocks; large asymmetric flows in latitude and longitude; large latitude and longitude extent of shocks; the importance of pre- and post- event solar background; and the importance of space weather throughout the heliosphere.

SPACE WEATHER AT ACE AND ULYSSES

Our model inputs SS maps to generate the background SW, and we have separate inputs for perturbing the BCs to represent solar events. Our approach is based on accurate reproduction of the SW consequences, not prediction. Our shock simulation inputs are applied near the top of the corona, a region of space that is poorly observed. Our first estimates of shock inputs come from the available space- and ground- based observations of solar events. Due to large uncertainties, these shock inputs usually do not result in close agreement between simulated and observed time series at various spacecraft (s/c). We, thus, apply an iterative tuning procedure [1, 2] to make the simulated shock arrival times agree with those observed. When s/c shock arrivals are correctly paired with solar events and the event inputs are so tuned, we get overall good agreement between the model and the data as shown in Figure 1. Here HHMS-PI was tuned in the iterative procedure using the solar inputs obtained by tuning the HHMS-PI shock arrival times to those observed at both ACE and Ulysses [1, 2]. Figure 1 shows the comparisons of our HHMS-PI simulation with ACE SW plasma speeds, densities, and temperatures, and the IMF orientation (Br-Bφ). We make our comparisons quantitative. We define [1, 2] and use the skill, also known as Prediction Efficiency, as: PE=1–MSE/VAR where MSE is the mean squared error and VAR is the variance of the observed time series. We also use the more familiar standard correlation coefficients (corr) between simulated and observed variables. Our consistent methodology has enabled explicit study of shock deceleration and interactions with other shocks (including from other flares, coronal mass ejections, corotating interaction regions), and with the

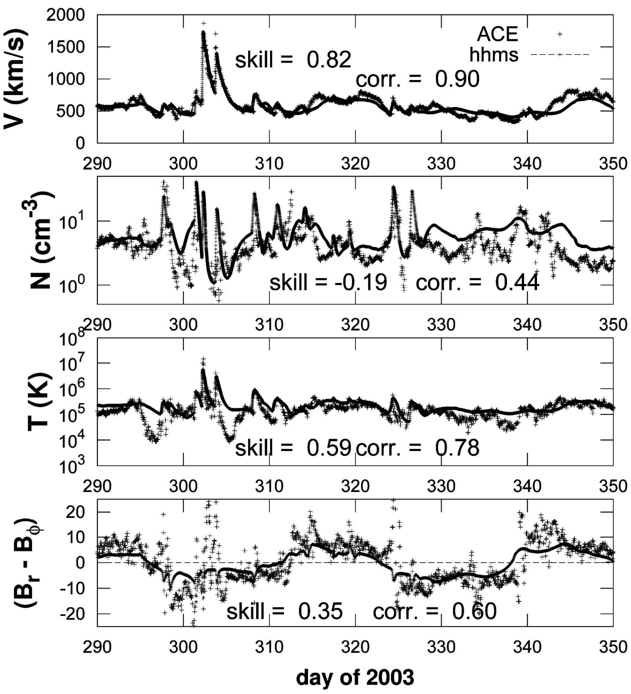

Fig. 1. HHMS-PI (smoother line), ACE (+): V, N, T, and (Br-Bφ) for Halloween 2003 solar events. Note that skill and correlation scores for V are 0.82 and 0.90.

heliospheric current sheet (HCS) and their global deformations at any latitude (within +/- 65°).

In 2004, we suggested [4] that OH dynamics (as measured by V1 and V2) may be very influenced by shocks of solar event origin as they asymmetrically propagate outward through the 3D SW. Our subsequent work has substantiated these results. Space weather originating on the Sun is responsible for much of the SW, particle, and field dynamics and characteristics throughout the heliosphere.

Table 1. Shock Arrival Delays at Ulysses Due to Pickup Protons (all day of 2003).

FF	DOYSUN	OBSULY	DNH_0 = 0.1	DNH_0 = 0	DIFF (days)
514	301.460	311.801	312.632	311.877	**0.755**
517	306.718	316.884	317.876	317.000	**0.876**
520	308.822	317.641	318.194	317.491	**0.703**
520.2	311.664	319.000	319.167	318.600	**0.567**
521	315.566	326.851	327.004	326.105	**0.899**
524	322.324	333.810	335.145	334.534	**0.611**

FF ⇒ Fearless Forecast event sequence number; DOYSUN ⇒ FF solar event day of 2003;
OBSULY ⇒ observed shock arrival at Ulysses day of 2003;
$DNH_0 = 0.1$ ⇒ simulated Ulysses shock arrival time for the case of neutral H density at ∞ = 0.1 cm^{-3};
$DNH_0 = 0$ ⇒ simulated Ulysses shock arrival time for the case of neutral hydrogen density equal to 0;
DIFF ⇒ ($DNH_0 = 0.1 - DNH_0 = 0$). Note: Positive values of DIFF demonstrate shock slowing due to inflowing neutral hydrogen

In [1] the specific effect of PUPs on shock propagation was quantified (see Table 1) by comparing two HHMS-PI runs to Ulysses, at 5.2 AU. The runs were identical except that in one the neutral H density was 0.1 cm^{-3} and in the other it was zero. The result was that the presence of PUPs caused the delay of all the shocks reaching Ulysses (see Table 1). The average delay was 17.6 hours. At ACE we found no differences in the shock arrival times. These results are consistent with our expectations. As we improve our PUP modeling, such agreements will increase between the observed and modeled shock arrivals. The analysis, based on Table 1, is fruitful since it shows for the first time the effects PUPs can have on shock propagation.

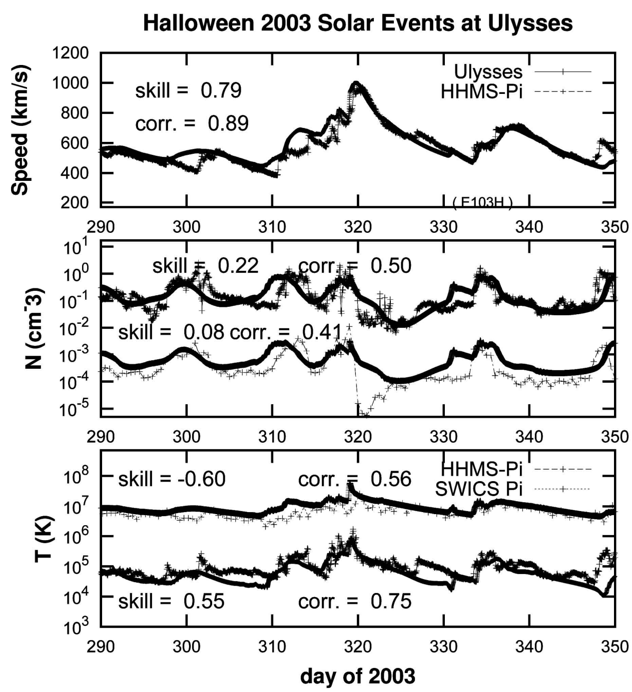

Fig 2. Comparison of HHMS-PI simulation (smoother line) with SWICS pickup proton (PUP) data (individual data points) at Ulysses [2]. Ulysses SWICS PUP measurements are courtesy of the Gloecklers.

Our success with the PUP modeling also is shown in Figure 2 [2] by the overall good agreement of our HHMS-PI simulation with Ulysses SW plasma speed, SW and PUP densities, and temperatures. At times the observed plasma distributions were changing drastically, giving rise to uncertainties in the parameters derived from the data [2]. There is one notable, large error in our PUP density where we missed the sudden drop in PUP density on day 320, coincident with the peak in SW speed. We believe [2] this is an example of the time-dependent physical process that we call "sweeping out". Our current stationary neutral H model cannot model any such time-dependent process. The time-dependent kinematic neutral H model we are planning to implement, by imposing mass conservation on the neutral H, would include the "sweeping out" physics, and thus it would either refute or support and refine the sweeping out dynamics.

Last year [5] we presented some additional results from our HHMS-PI modeling of the Halloween solar events out to 75 AU. These results showed that space weather arising from the Sun propagates throughout the heliosphere. The large latitude and longitude asymmetries associated with these events in the OH and their large latitude and longitude extent in the OH are additional evidence of the dynamic effects of space weather throughout the heliosphere. Webber and Intriligator (2011) [6] showed that the location and shape of the termination shock (TS) and of the heliopause may be directly related to space weather conditions emanating from the Sun.

SPACE WEATHER AT VOYAGER 2

We reported [7] the presence of elevated readings ("High Energy Ions (HEIs")) in the V2 Plasma Subsystem (PLS) [8] data near the TS crossings at 84 AU. These elevated readings occurred on energy/charge (E/Q) step 12 (= 554 km/s for protons) on the PLS B-Cup [7]. Now since we do not know the source of the elevated B12 readings - and, as discussed below, at times there may be several sources - we will refer to them as "elevated B12 readings" rather than "HEIs" [7]. The PLS has four cups: the A-, B-, and C-Cup face the solar direction and the D-Cup looks perpendicular to the solar direction [8, 7]. The V2 Plasma Wave Subsystem [9, 10] detected plasma waves near the TS, which we [7] suggested were due to a two-stream ion instability [9] between the convective heliosheath (HS) plasma flow and the HEIs

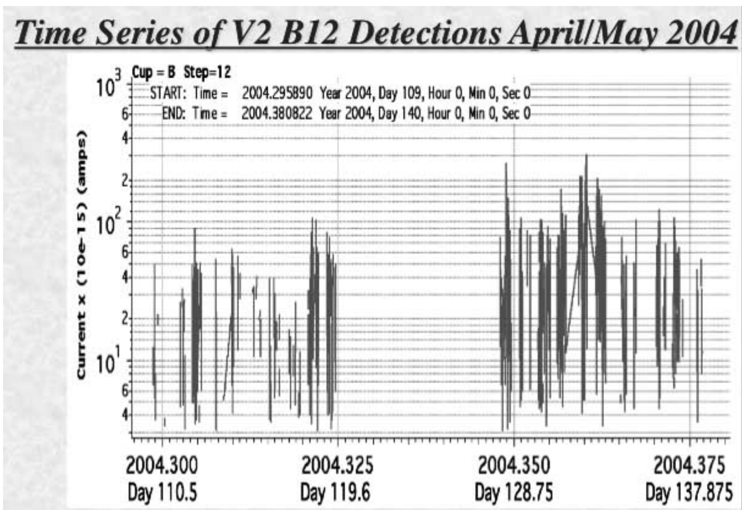

Figure 3. Time series of V2 PLS elevated B12 readings. There are two intervals of elevated B12 readings. The first interval includes the smaller IP shock (~ Day 110, see Figure 5) and extends to ~Day 119.6. The larger IP shock (see Figure 5) occurred later on Day 119 (during a gap in V2 data tracking). The second interval of elevated B12 currents began almost 10 days after the larger IP shock and had the higher elevated B12 readings, some of which may be due to the SW speed of ~ 550 km/s being measured on B-Cup at E/Q step = 12 which corresponds to a proton speed of ~ 554 km/s.

(B12s).

In the present paper we show evidence for the association of these elevated B12 readings with phenomena at V2 related to the interplanetary (IP) manifestations of the Halloween 2003 events. In early 2004 V2 was located at ~ 73.2 AU, 215.3° HGI heliographic longitude (Heliographic inertial coordinate system (NSSDC)), and South at 25.2° HGI latitude [11, 12]. We found two intervals of elevated B12 readings in the PLS data associated with the Halloween 2003 events in the V2 data [11, 13]. The first interval started at ~ 0500 UT on Day 109, 2004, about one day before the first IP shock arrival on ~ Day 110 [11], and intermittently continued for ~ 10 days until the data tracking gap during which the larger IP shock occurred on Day 119 [11, 13, 14]. The second interval of elevated B12 readings began on Day 128, about 9 days after the larger IP shock, and continued intermittently for ~ 11 days to Day 139. Figure 3 shows the timing of all of these elevated B12 readings and their magnitudes.

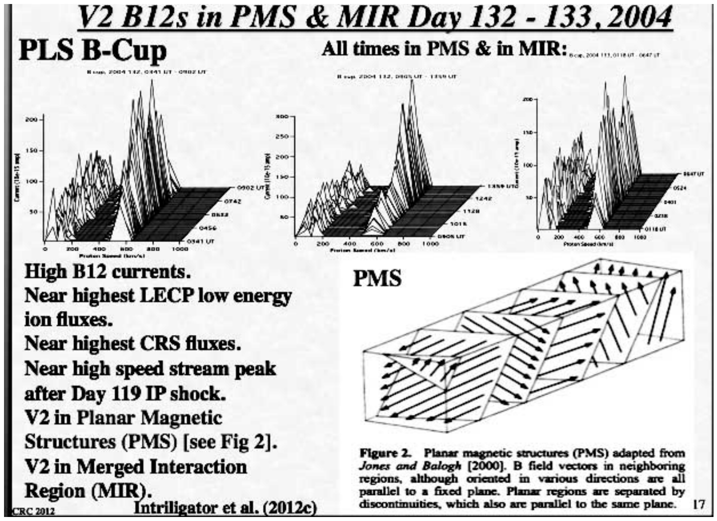

Figure 4. V2 PLS E/Q spectra observed in PMS and MIR on Day 132-133. The elevated B12 currents are the higher currents - shown on the right - in each spectrum. The inset on left [8] illustrates the IMF geometry in PMS.

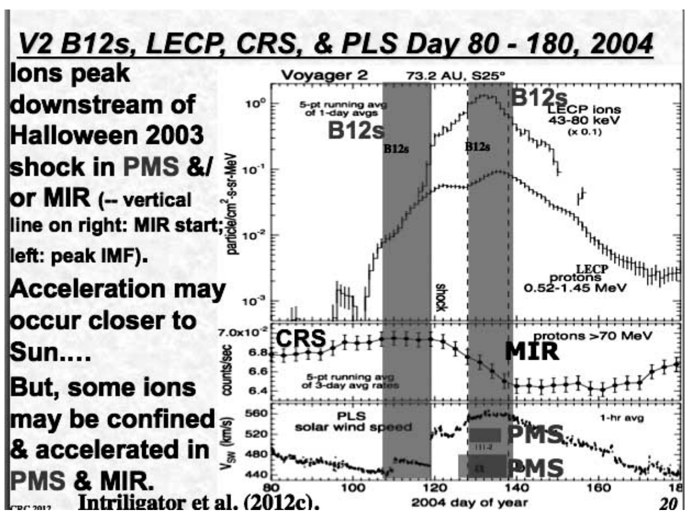

Figure 5. V2 elevated B12 readings (shaded vertical bands), LECP ion data, CRS > 70 MeV (note Forbush decrease), PLS SW speed, larger IP shock (vertical solid line), start of MIR (left vertical dashed line), the two PMS (horizontal bars), and the peak IMF (right dashed line).

The most intense elevated B12 readings were observed on Days 128-133, about 9-14 days after the larger IP shock on Day 119. The elevated B12 readings, shown in Figure 4, are the most intense V2 elevated B12 readings we have found. This includes the elevated B12 readings in the OH, near the V2 TS crossings at 2007.6, near the end of 2007 after the TS crossings, and in the HS. In Figure 4 to more clearly show the elevated B12 reading portion of the B-Cup spectra, the current ranges of the vertical axes vary between the various sets of B-Cup spectra. The inset in Figure 4 is from [12] and shows a schematic sketch of Planar Magnetic Structures (PMS) with the various planar structures parallel to a fixed plane. For the Halloween events at V2 we [12] identified two PMS time intervals: A (Day 125.8-138.2, 2004) and B (Day 131.2-137.8.)

The two intervals of elevated B12 readings are shown by the two shaded vertical bands in Figure 5. The larger IP shock is shown by the solid vertical line in Figure 5. The most intense elevated B12 readings in Figure 4 were near the PMS [12] and the Merged Interaction Region (MIR) [14]. The MIR extended from Day 128-167 [14]. The shaded horizontal bars in Figure 5 denote the two PMS intervals. In Figure 5 the start of the MIR is shown by the vertical dashed line on the left, and the time of maximum IMF magnitude is shown by the vertical dashed line on the right [14]. Figure 5 also shows the SW speed [13], the Forbush decrease in the > 70 MeV proton CRS data [16], and some peaks in the LECP ion data [15].

The two V2 intervals of elevated B12 readings also coincided with low energy ion detections in the V2 LECP data [15] and of peak particle intensities in the V2 CRS data [16]. Figure 5 shows that the highest elevated B12 readings (Figure 4) corresponded to the peak LECP ion readings, the CRS Forbush decrease, the highest SW speeds, and the peak IMF value. During this time the PLS showed [14] that with the arrival of the larger IP shock on Day 119 there was a jump then a decrease in SW speed and then the speed continued to increase, as shown in Figure 5, until ~ Day 133 when the speed was ~ 550 km/s. The proton speed associated with E/Q step 12 is 554 km/s [7]. Thus, on Days 128-133 some of the peak elevated B12 readings may be associated with the bulk SW speed near ~550 km/s. This is discussed in more detail in [18]. The other (i.e., not SW) elevated B12 readings may be tracers, indicators, or by-products of important physical processes (e.g., proton pickup, particle acceleration, turbulence, etc.). This appears to be the case for our previously reported [7, 17] elevated B12 readings, and for the first interval reported here, and also to some extent for the second interval reported here.

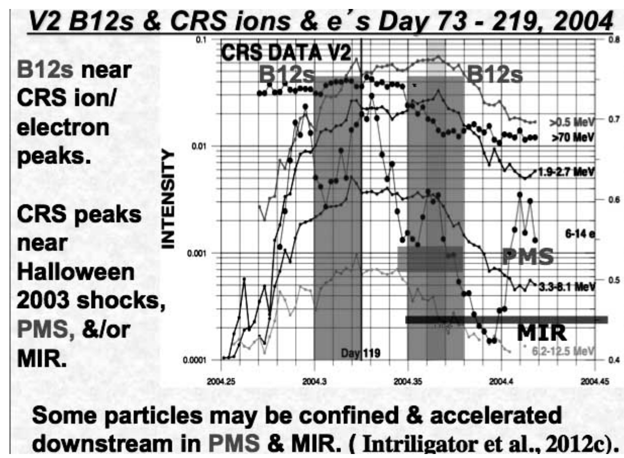

Figure 6. V2 elevated B12 readings (vertical shaded bands) and CRS ion and electron data. PMS (thicker horizontal bar) and MIR (longer narrower horizontal bar) are also shown.

Figure 6 summarizes additional CRS data in the context of the elevated B12 readings and the IMF. The two vertical shaded bands again denote the intervals of elevated B12 readings, the thicker shaded horizontal bar the PMS, and the longer narrower horizontal bar the MIR. A well-defined increase in the CRS 6-14 MeV electrons (shown by the grey vertical band) occurred during the second interval of elevated B12 readings, near the peak CRS > 0.5 MeV proton readings in the PMS. This electron increase is also near the IMF peak in the MIR. Comparisons of the LECP 43-80 keV ion and 0.52-1.45 MeV proton data in Figure 5 with the CRS peak

>0.5 MeV proton and 6-14 MeV electron data in Figure 6 appear to indicate that they all peak near the same time. This time interval also corresponds to the higher elevated B12 readings in the second shaded vertical band, the higher SW speed (Figure 5), and the peak IMF magnitude (the right dashed vertical line in Figure 5). They all occurred in the PMS and in the MIR.

Figure 7 summarizes measurements from four V2 instruments and indicates additional information about IP characteristics during this time. The bottom panel in Figure 7 shows the broad peaks covering many days (~ Day 108-142) in the CRS proton data in the 2-3 and 3-8 MeV energy ranges. The second panel from the bottom shows the LECP electron data in the 22-35 & 35-61 keV range. Unlike the broad peaks in the CRS proton data, these LECP electron data indicate a narrower peak in electron counts that occurred before the largest proton peak. This electron peak occurred closer to the large shock (Day 119) and peaked near Day 125. In contrast, the CRS protons and LECP ions (in Figure 5 and in the third panel (28-43, 43-80 keV, 0.54-1.0 MeV) from the bottom in Figure 7) peak near Day 135. The elevated B12 readings are shown in the fourth panel from the bottom. Comparison of the elevated B12 readings with the CRS and LECP data indicates that the LECP peak electron data primarily occurred from the start of the first interval of elevated B12 readings and extended to the end of the second interval of elevated B12 readings with the highest LECP electron data occurring in the gap between the two intervals of elevated B12 readings (i.e., where there are no elevated B12 readings). The top two panels in Figure 7 show IMF components: the second panel shows Bphi (direction angle in degrees) and the top panel shows Br (nT). We note the first interval of elevated B12 readings followed an IMF rotation (Bphi changing from + to -). This first interval of elevated B12 readings ended when Bphi had a smaller rotation and when Br changed from – to +. During the gap between the two intervals of elevated B12 readings both IMF components showed ~sinusoidal variations. These variations, particularly in Br, continued beyond the second interval of elevated B12 readings. The start of the second interval of elevated B12 readings coincided with an increase in Br and a decrease in Bphi. It is tempting to associate the Br rotations with an acceleration process, e.g., magnetic reconnection, magnetic pumping, etc. Figure 8 shows a V2 LECP ion spectrum and an electron spectrum that were measured on Day 118. Note the similar shape of the two spectra. The larger IP shock arrived on Day 119.

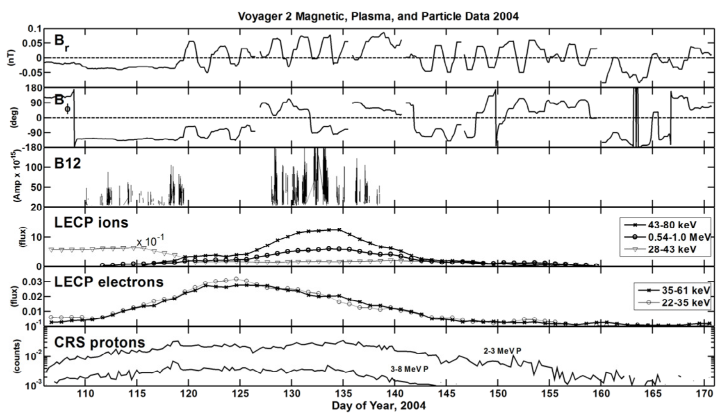

Figure 7. V2 CRS protons (bottom panel); LECP electrons (2nd panel from bottom) and protons (3rd panel from bottom); PLS elevated B12 readings (4th panel from bottom); IMF Bphi (2nd panel from top) and Br (top panel).

While it is also tempting to associate the V2 elevated B12 readings near the Halloween 2003 IP shocks with PUPs, this may not be the case for both intervals of elevated B12 detections. One expects the PUP distribution during the first interval of elevated B12 readings to extend in speed from 0 to ~ 960 km/s (twice the SW speed at this time) and not to manifest itself at ~ 554 km/s. In the second interval of elevated B12 readings the reported SW speed reached ~550 km/s, implying the PUP distribution during the second interval might extend from 0 to ~1100 km/s.

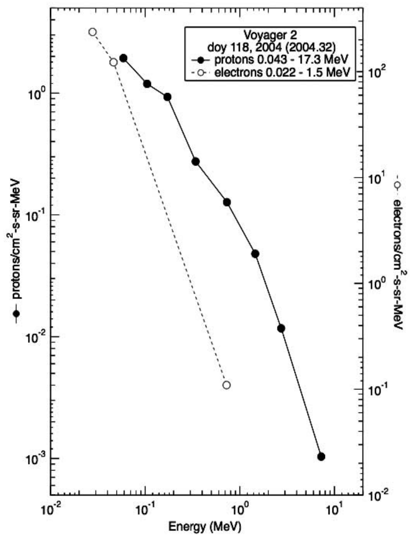

Figure 8. LECP ion and electron spectra on Day 118. The Halloween 2003 IP shock passed V2 during data gap on Day 119.

It appears that the origin of some of the elevated B12 readings at 550 km/s (e.g., on Day 128, 132, and 133) may have a different origin than the first interval of elevated B12 readings in 2004, or than those near the TS, etc. We believe that on Day 128, 132, and 133 some of the elevated B12 readings may be due to the B-Cup detecting the bulk SW protons at the speed of ~550 km/s [18]. Thus, at V2 in association with the IP Halloween 2003 events it appears that the elevated B12 readings during the first interval and some of the elevated B12 readings during the second interval may be evidence of PUPs, particle acceleration, or of other processes. Whereas, during the second interval of elevated B12, some of these readings are attributable to the increase in the bulk SW speed to ~ 550 km/s. Our comparisons of the simultaneous V2 data from many instruments indicate that there is evidence of simultaneous variations in the V2 particle and field data that may be indicative of acceleration and/or turbulence occurring near the shocks, in the PMS, and in the MIR. Some of the plasma and particles in the PMS may have been trapped there for relatively long times and were undergoing acceleration over relatively large distances as the PMS propagated outward in the heliosphere. Other plasma and particles in the PMS may have undergone local acceleration more recently, i.e., closer to their times of detection. While we do not know unambiguously the source(s) of the two intervals of elevated B12 readings associated with the Halloween 2003 IP shock propagation, we do know that they appear to be indicators, signals, or tracers of significant physical processes occurring in the IP near V2. The analyses we presented here of the V2 data associated with the IP Halloween 2003 events appear to indicate that there may be many diverse affects of space weather throughout the heliosphere.

ACKNOWLEDGMENTS

The work at Carmel Research Center was supported in part by NASA grant NNX08AE40G and by Carmel Research Center, Inc. The work at NMSU and at APL was supported by the VIM. We are grateful to John Richardson and John Belcher for the PLS data, George Gloeckler and Christine Gloeckler for the Ulysses SWICS PUP data, the NSSDC for the ACE, Ulysses, and V2 SW and IMF data, and to Ed Sittler and Ralph McNutt for discussions of the PLS data.

REFERENCES

1. T. R. Detman, D. S. Intriligator, M. Dryer, W. Sun, C. S. Deehr, and James Intriligator, The influence of pickup protons, from interstellar neutral hydrogen, on the propagation of the interplanetary shocks to ACE and Ulysses from the Halloween 2003 solar events: A 3D MHD modeling study, *J. Geophys. Res., 116,* A06105, doi: 10.1029/2010JA015803, 2011.
2. D. S. Intriligator, T. Detman, G. Gloeckler, C. Gloeckler, M. Dryer, W. Sun, J. Intriligator, and C. Deehr, Pickup protons: Comparisons using the three-dimensional MHD HHMS-PI model and Ulysses SWICS measurements, *J. Geophys. Res.,* 117, A06104, doi:10.1029/2011JA017424, 2012a.
3. C. N. Arge, and V. J. Pizzo, Improvement in the prediction of solar wind conditions using near real time solar magnetic field updates, *J. Geophys. Res., 105*, 10,465-10,479, 2000.
4. D. S. Intriligator, M. Dryer, W. Sun, C.D. Fry, C. Deehr, and J. Intriligator, Dynamics of the Outer Heliosphere, *Physics of the Outer Heliosphere,* V. Florinski, N. Pogorelov, and G. Zank eds, 117-126, AIP Conference Proceedings 719, 2004.
5. D. S. Intriligator, T. R. Detman, M. Dryer, J. Intriligator, W. Sun, W.R. Webber, and C.S. Deehr, Insights Gained From the Propagation of the 3D MHD Time-Dependent HHMS-PI (Hybrid Heliospheric Modeling System with Pickup Protons) from the Sun to Voyager 2: The Halloween 2003 Solar Events, AIP Conf. Proc., 1436, Eds. Zank, Heerikhuisen, Li, &Pogorelov, pp. 314-320; doi:http://dx.doi.org/10.1063/1.4723625, 2012b.
6. W. R. Webber and D. S. Intriligator, Voyagers 1 and 2 in a shrunken and squashed heliosphere, *J. Geophys. Res*., 116, A07107, doi: 10.1029/2011JA016478, 2011.
7. D. S. Intriligator, J. Intriligator, W. D. Miller, and W. R. Webber, Higher energy plasma ions found near the termination shock: Analyses of Voyager 2 data in the heliosheath and in the outer heliosphere, J. Geophys. Res., 115, A07107, doi: 10.1029/2009JA014967, 2010.
8. H.S. Bridge, J.W. Belcher, R. Butler, A.J. Lazarus, A.M. Mavretic, J. D. Sullivan, G.L. Siscoe, and V.M. Vasyliunas, The plasma experiment on the 1977 Voyager mission, Space Sci. Rev., 21, 259-287, 1977.
9. D. Gurnett and W. Kurth, *Nature 07023, 454*, doi:10.10.38, 2008.
10. D.A. Gurnett, W. S. Kurth, L.F. Burlaga, M. H. Acuna, N.F. Ness, J.D. Richardson, and N. Omidi, Electrostatic waves observed at and near the solar wind termination shock by Voyager 2, in Particle Acceleration and Transport in the Heliosphere and Beyond, 7th Annual International Astrophysics Conference, AIP 1039, page 335 - 342, 2008.
11. D. S. Intriligator, W. Sun, M. Dryer, C. D. Fry, C. Deehr,' and J. Intriligator, From the Sun to the Outer Heliosphere: Modeling and Analyses of the Interplanetary Propagation of the October/November (Halloween) 2003 Solar Events, *J. Geophys. Res.,* 110(A9), A09S10, doi:10.1029/2005JA010939, 2005.
12. D.S. Intriligator, A. Rees, and T. S Horbury, First analyses of planar magnetic structures associated with the Halloween 2003 events from the Earth to Voyager 1 at 93 AU, *J. Geophys. Res.,* 113, A5, doi:10.1029/2007JA012699, 2008.
13. J.D. Richardson, C. Wang, J.C. Kasper, and Y. Liu, Propagation of the October/November 2003 CMEs through the Heliosphere, *Geophys. Res. Lett.,* 32, doi: 10.1029/2004GL020679, 2005.
14. L. F. Burlaga, N. Ness, E.C. Stone, F.B. McDonald, & J. Richardson, Voyager 2 observations related to the October-November 2003 solar events, *GRL, 32*, L03S05, doi:10.1029/2004GL021480, 2005.
15. R. Decker, S. Krimigis, M. Hill, T. Armstrong, G. Gloeckler, D. Hamilton, and L. Lanzerotti, *Nature 07030*, 454, doi:10.10.38, 2008.
16. E.C. Stone, et al. (1977), Cosmic ray investigation for the Voyager missions: energetic particle studies in the outer heliosphere – and beyond, Space Sci. Rev., 21, 355-376 doi: 10.1007/BF00211546.
17. D. S. Intriligator, J. Intriligator, W. D. Miller, W. R. Webber, R. B. Decker, W. Sun, T. Detman, M. Dryer, and C. Deehr Voyager 2 high energy ions near the outward moving termination shock, AIP Conf. Proc., 1352, 148-157, Eds. Le Roux, Florinski, Zank and Coates, 2010.
18. D. S. Intriligator, J. Intriligator, W. D. Miller, W. R. Webber, R. B. Decker, E. C. Sittler, R. McNutt, R. L. McPherron, et al., preprint, 2012c.